JMEPEG (2008) 17:864–869
DOI: 10.1007/s11665-008-9238-0

1059-9495/$19.00

A New Continuous Cooling Transformation Diagram for AISI M4 High-Speed Tool Steel

Jalel Briki and Souad Ben Slima

(Submitted January 5, 2007; in revised form March 10, 2008)

The increasing evolution of dilatometric techniques now allows for the identification of structural transformations with very low signal. The use of dilatometric techniques coupled with more common techniques, such as metallographic, hardness testing, and x-ray diffraction allows to plot a new CCT diagram for AISI M4 high-speed tool steel. This diagram is useful for a better selection of alternate solutions, hardening, and tempering heat treatments. More accurate determination of the various fields of transformation of austenite during its cooling was made. The precipitation of carbides highlighted at high temperature is at the origin of the martrensitic transformation into two stages (splitting phenomena). For slow cooling rates, it was possible to highlight the ferritic, pearlitic, and bainitic transformation.

Keywords carbide precipitation, continuous cooling diagram, dilatometry, heat treating, M4, splitting phenomena, tool steels

1. Introduction

High-speed tool steels are generally used for tools subjected to high temperature and mechanical stresses for cutting of metallic materials. The properties of high-speed steels develop as a result of adequate heat treatments resulting in a good combination of high hardness and adequate toughness in the material.

Knowing what will occur during a heat treatment, and specifically during the cooling process, can guide designers in selecting the appropriate heat treatment for the desired application. This is the role of continuous cooling transformation (CCT) diagrams. We present in Fig. 1, the only chart published and shown on the data sheet steel studied (Ref 1). This diagram shows a lack of precision on the one hand, the extension of the precipitation of carbides (the beginning of this transformation are represented by the dotted line (C), and their purpose are not at all represented). On the other hand, the limits on the bainitic domain (line B) lacked precision in its left side.

The determination of CCT diagrams is directly dependent on the dilatometric techniques to determine the different transformation temperatures during cooling. Fortunately, dilatometry has made significant progress in sensitivity and precision of the technique in recent years (Ref 2). Thus, it is now possible to detect minor transformations that induce very low dimensional changes in materials such as the precipitation of very small carbide particles.

The aim of this study is to propose a new CCT diagram that more accurately represents the microstructural evolution of AISI M4 tool steel during cooling from an austenitization temperature of 1220 °C.

Jalel Briki and **Souad Ben Slima**, Mechanical Department, Engineering School of Tunis, Tunis, Tunisia. Contact e-mail: jalel.briki@enit.rnu.tn.

2. Material and Experimental Procedure

2.1 Material

The AISI M4 tool steel used in this study was fabricated by Erasteel Company (Ref 1). It is received in the form of round bar of diameter 30 mm. Melting was carried out with electroslag remelting (ESR) process. After hot working and hot stripping, material is annealed. The composition of the as-received material is shown in Table 1. The C and S contents have been verified using conventional LECO C and S analysis. The austenitizing temperature is 1220 °C that is generally used in industry.

2.2 Experimental Procedure

For this study, two different dilatometers were used depending on the cooling rate from austenitization temperature. For relatively low cooling rates of 0.08 to 0.007 °C/s, an ADAMEL model DI24 dilatometer was used. This dilatometer is fully computer controlled allowing for digital experimental control, data collection, and analysis. For relatively high cooling rates of 0.1 to 200 °C/s, an ADAMEL model DT1000 dilatometer was used. All thermal analysis samples were cooled by He(g). Sample dimensions were 5 mm diameter and 25 mm length, and 2 mm diameter and 12 mm length for use in the DI24 and DT1000 dilatometers, respectively.

Observations of the tool steel microstructure have been performed using both optical and scanning electron microscopy. Analyses of carbides have been conducted using secondary, backscattering electron and energy dispersive spectrum analysis (EDS) on the scanning electron microscope (SEM). Samples have been metallographically ground, polished, and then etched using a Nital etchant (Ethanol + 5 vol.% Nitric acid) to reveal the microstructure. Constituent phase in tool steel samples were identified using a Siemens Kristalloflex

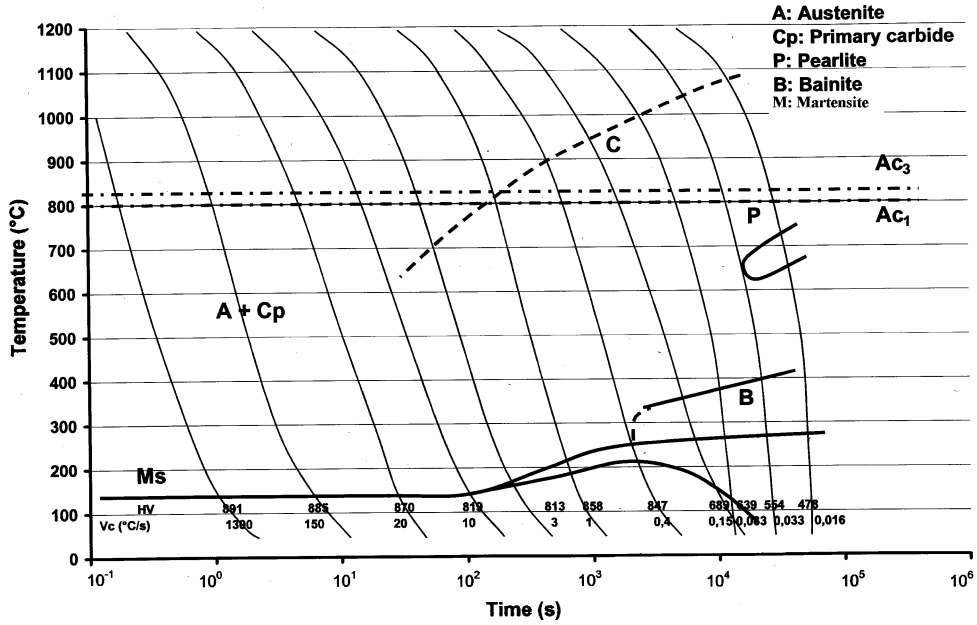

Fig. 1 The continuous cooling transformation diagram for AISI M4 high-speed tool steel reproduced with permission from the manufacturer

Table 1 Chemical composition of the steel studied

Elements	C	Cr	Mo	W	V	Mn	P	S
Weight percent	1.29	4.03	4.43	5.26	3.82	0.40	0.03	0.02

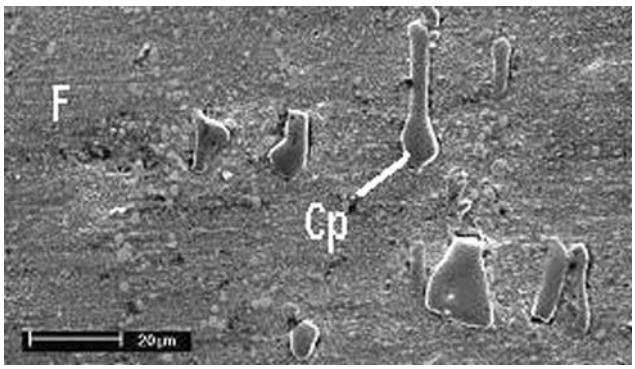

Fig. 2 SEM microstructure of M4 high-speed tool steel in the as-received condition (F: ferrite; Cp: primary carbide)

X-ray diffractometer with a Cu anode. The samples analyzed were either solid tool steel or carbides that had been chemically extracted from the tool steel matrix. Vickers hardness of tool steel samples was determined for the various continuous cooling rates using a 500 gm force.

3. Results and Discussion

3.1 The As-Received Condition

In the as-received condition (annealed), the M4 tool steel samples had a Vickers hardness of 270 HV which corresponds to a ferritic matrix (F) with dispersed carbides of varying forms

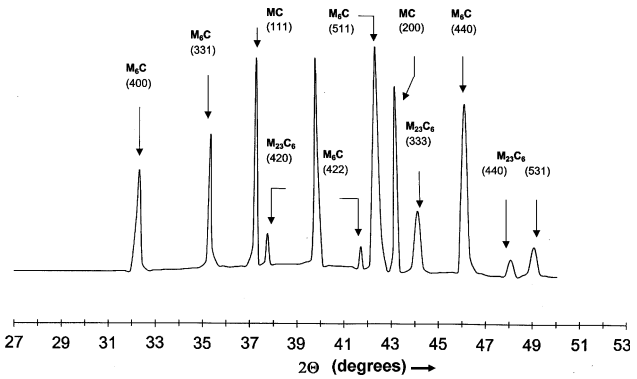

Fig. 3 X-ray diffraction pattern of carbides extracted from M4 tool steel in the as-received condition

and size, reaching up to 20 µm in size and aligned with the hot working direction (Cp) as shown in Fig. 2. The weight percentage of those carbides, identified, after the electrolytic extraction was 15%.

A typical x-ray diffraction pattern of extracted carbides is presented in Fig. 3. The analysis of this spectrum has enabled the identification of peaks as follows: MC (or M_4C_3), $M_{23}C_6$, and M_6C. Analysis of carbides by SEM-EDS with back scattered electron (BSE) imaging used for identifying the various carbides, shows (Fig. 4 and Table 2) that there are two main kinds of carbides: one with gray color is the V-rich carbide (A and B positions) with sizes of about 10-15 µm, another with white color is W-rich carbide with sizes of 1-5 µm. The carbides identified are those generally encountered in the high-speed tool steels (Ref 3-5).

Homogenization of the as-received M4 material at 1220 °C allows for partial dissolution of carbides and saturates the austenite matrix with C and other alloying elements. At 1050 °C $M_{23}C_6$ carbides are dissolved, whereas M_6C and MC carbides dissolve at still higher temperatures. The dissolution of

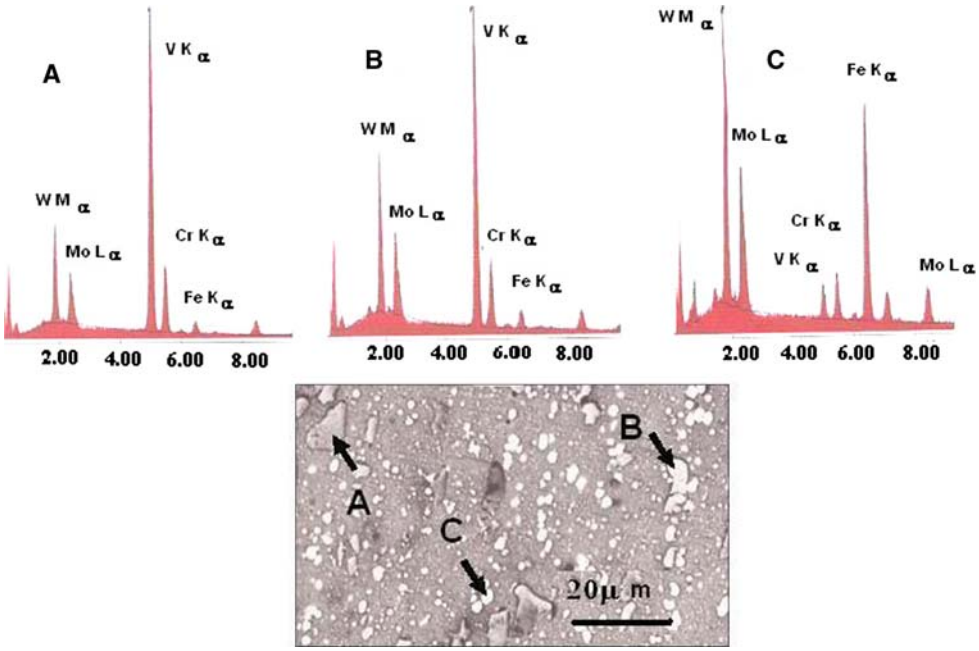

Fig. 4 SEM-micrograph and EDS analysis of carbides in as-received condition

Table 2 The composition (in mass %) of carbides marked A, B, and C in SEM micrograph of Fig. 4

	A	B	C
W	34.72	43.68	28.36
Mo	9.66	12.41	15.13
V	49.34	37.69	5.22
Cr	3.56	2.78	6.15
Fe	2.72	3.44	45.04

M_6C and MC carbides has been shown to occur at temperatures higher than 1220 °C (Ref 6-8). After homogenization at 1220 °C the M4 tool steel microstructure consists of an austenite matrix containing metal carbides.

3.2 Continuous Cooling Transformation Diagram

The construction of CCT diagram is performed as follows: once the transformations start and finish, reaction temperatures are determined for each cooling rate. These temperatures are superimposed on the corresponding cooling curve, which is plotted as temperature versus log time. Figure 5 presents a summary of dilatometer curves showing change in length per unit length plotted against temperature for the different cooling rates used in this study. The start and end temperature of austenite transformation has been followed by changes in slope observed on the curves recorded (dashed lines in Fig. 5). For better accuracy and for each of cooling rates, we used the recording derivative curves (Figs. 6 and 7). Furthermore, the different structures produced during the cooling of the austenite have been identified by microscopy (Fig. 8). On the other hand, the hardness measurements have enabled us to confirm the microstructures observed as well as domains of cooling rates characteristics.

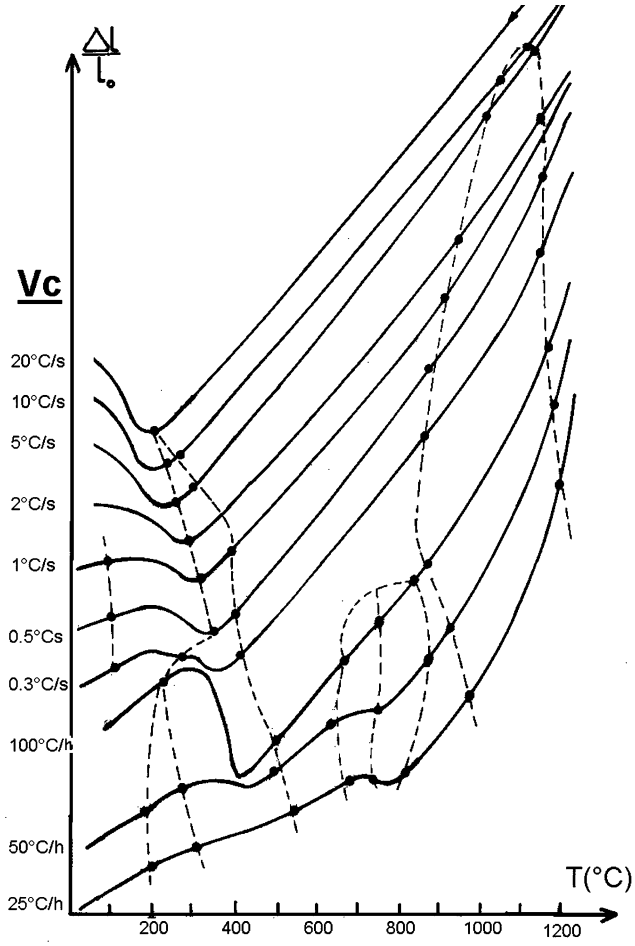

Fig. 5 Dilatometric curves for different cooling rates

The experimentally determined CCT diagram is presented in Fig. 9. Several observations can be made about what occurs during cooling for the different rates of cooling (Vc) used. Three cooling rate domains can be defined and are discussed below.

3.2.1 Domain I: Vc ≥ 15 °C/s. The dilatometer curve for cooling rate of 20 °C/s shows only one expansion due to the martensitic transformation and this is seen to occur at 190 °C. The end of this transformation is obtained when cooling is extended to low temperatures. Figure 10 indicates dilatometric behavior when the sample is cooled in liquid nitrogen on which we noted a point temperature Mf = −90 °C. This same curve has allowed us to estimate the volume fraction of nontransformed austenite using the method of IRSID (Ref 9). The volume fraction of retained austenite is about 15%.

3.2.2 Domain II: 0.2 °C/s ≤ Vc < 15 °C/s. As shown in the dilatometer curves of Fig. 4 (in example Vc = 0.2 °C/s) and of Fig. 8b for Vc = 1 °C/s, both a high-temperature carbide precipitation and two temperatures of Martensitic

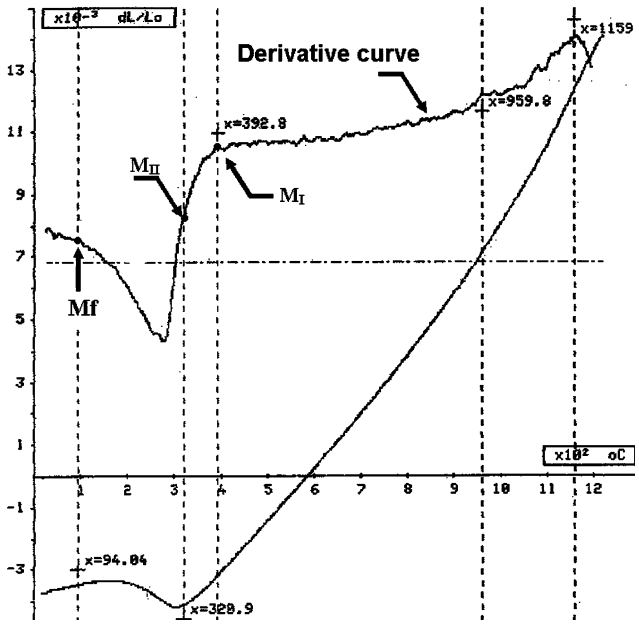

Fig. 6 Dilatometric with their derivative curve for Vc = 1 °C/s

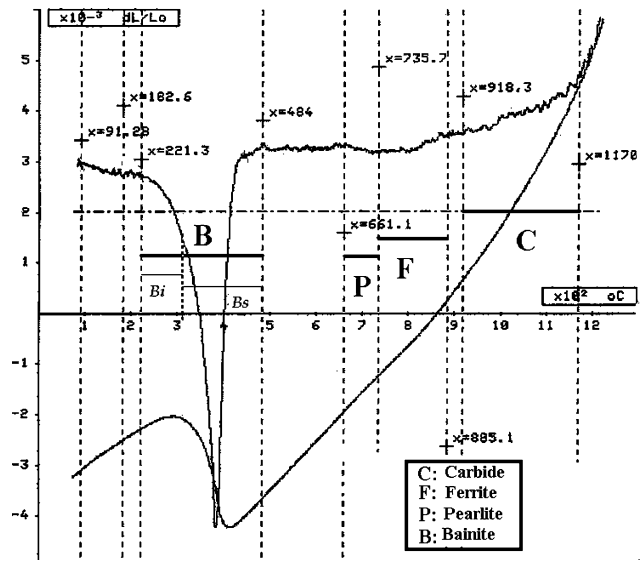

Fig. 7 Dilatometric with their derivative curve for Vc = 100 °C/h

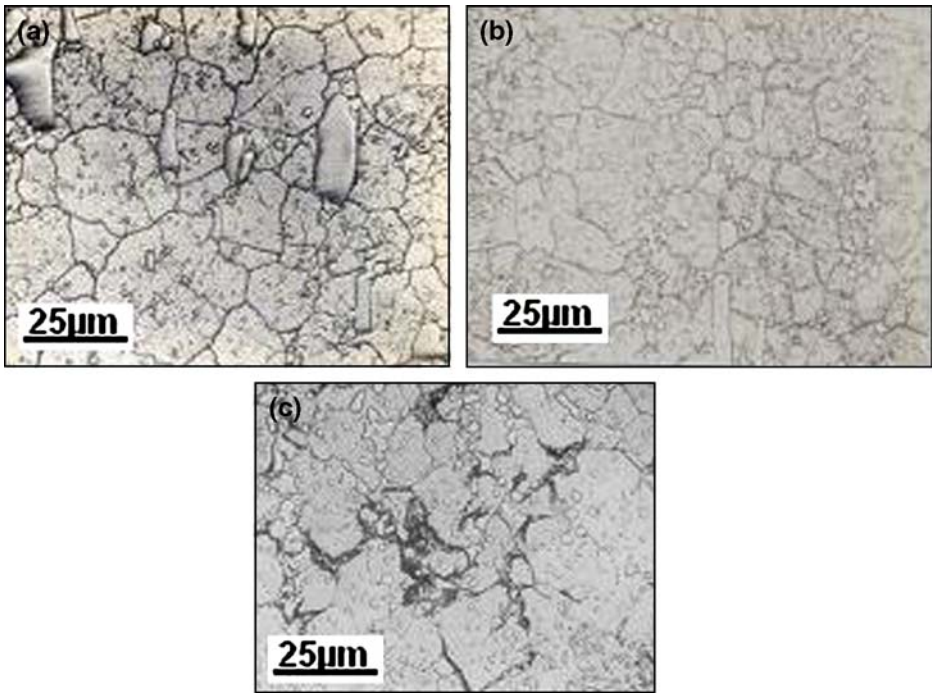

Fig. 8 Microstructure obtained after cooling rate: (a) 20 °C/s, (b) 2 °C/s, (c) 50 °C/h

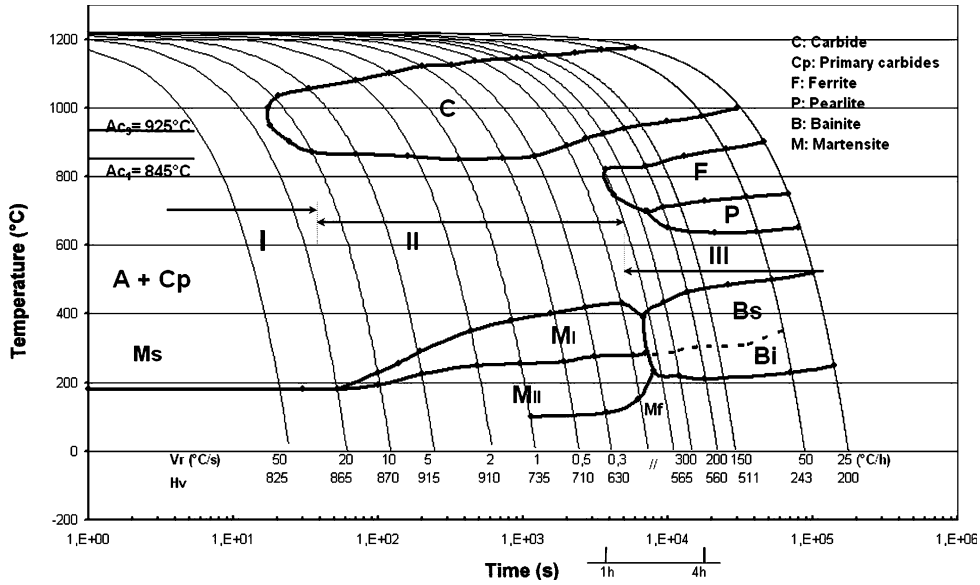

Fig. 9 CCT diagram for M4 HSS austenitized at 1220 °C

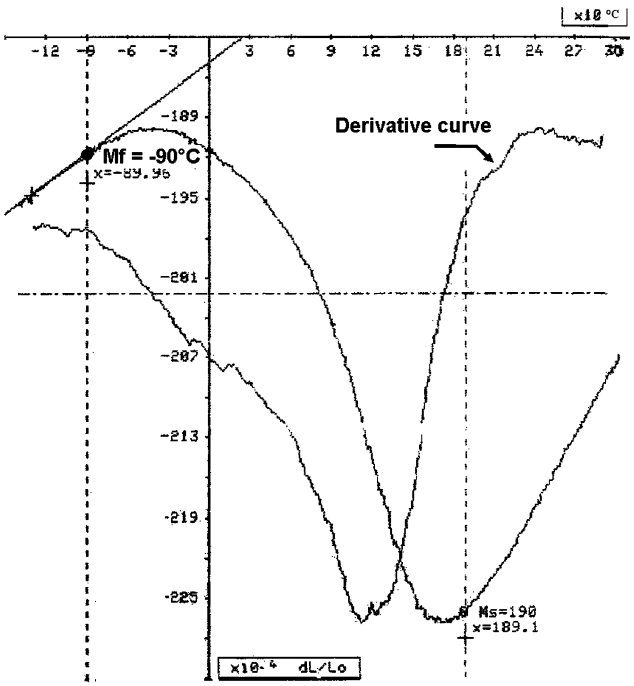

Fig. 10 Dilatometric behavior when sample is cooling in N_2 (l) media

transformation start (MI and MII) occur. The presence of two Ms temperatures is known as the splitting phenomena and is due to a decrease in alloy content such as at the carbide-matrix interface. For M4 steel of this study, the splitting phenomena are manifested by an increase in Ms to 200 °C ≤ MI < 420 °C (Ref 2, 10).

For the austenite-to-martensite transformation that occurs at MI, the transformation product is mainly martensite. Because of the carbon and alloying element impoverishment in austenite resulting from the significant carbide precipitation, the end of martensitic transformation occurs at relatively high temperature Mf ≥ 90 °C as shown in cooling curves for Vc = 1, 5, and 0.3°C/s in Fig. 4.

3.2.3 Domain III: Vc ≤ 0.2 °C/s. At relatively low cooling rates after carbide precipitation has occurred, the transformation of austenite to ferrite and pearlite (dark regions in Fig. 8c) is possible. This transformation is shown in the dilatometer curves of Fig. 4 for 100, 50, and 25 °C/h. At lower temperature, the bainitic transformation of austenite takes place. The dilatometric recordings have allowed us to distinguish two stages, which give successively the upper and the lower bainite (see Bs and Bi in dilatometric curve of Fig. 7). This distinction needs to be confirmed by other techniques; that is why their borders were made in dashed line in Fig. 9.

Overlaying diagram obtained in this study with those obtained industrially (dashed line in Fig. 11) allows us to identify significant differences. The field of carbide precipitation at high temperature is much better defined and temperatures indicating start precipitation of carbides prove to be higher. The presence of two distinct areas substantially corresponds to the transformation of austenite by diffusion to ferrite and then pearlite.

In the new CCT diagram, the beginnings of martensitic transformation, as well as the field of splitting phenomena, take place at higher temperatures; we were also able to detect the end of martensitic transformation (Mf in Fig. 11) for cooling rates between 1 and 0.3 °C/s. Finally, the area of the austenite-to-bainite transformation is better defined (upper and lower bainite, successively Bs and Bi in Fig. 11).

4. Conclusion

We present in this work a new route of continuous cooling transformation diagram of the AISI M4 high-speed steel. When the cooling rate is greater than 15 °C/s, the transformation of austenite is incomplete and proceeds to form martensite. For medium cooling rates (between 0.2 and 15 °C/s), the first product is austenite carbide, and then as the temperature

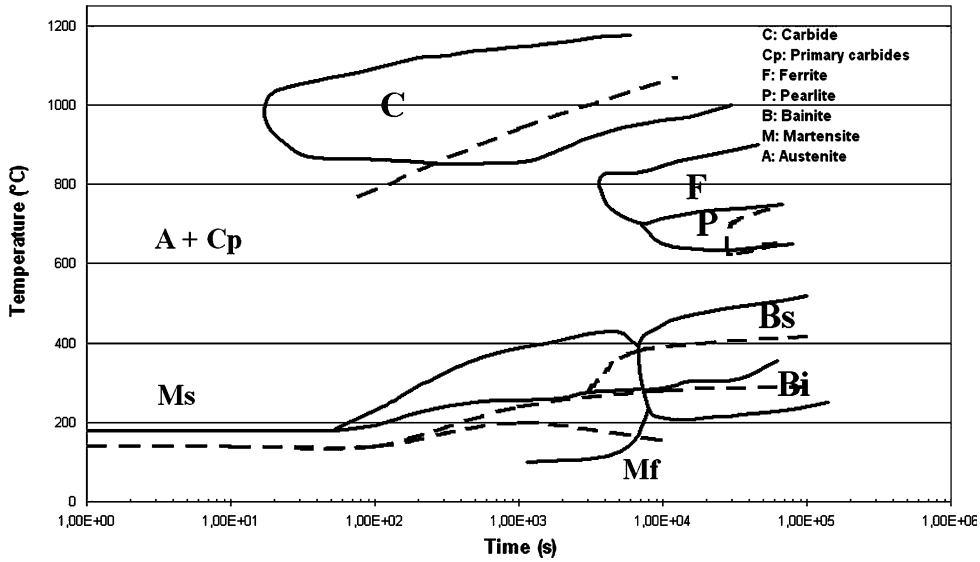

Fig. 11 Comparison between the diagram obtained in this study with that of the manufacturer

decreases, it turns into martensite. For this range of cooling rate, martensite transformation splits into two stages identified by high-resolution dilatometry. For cooling rates lower than 0.2 °C/s, in addition to carbide precipitation, the transformation of austenite by diffusion take place and it gives successive phases ferrite and pearlite; after that, the nontransformed austenite produces bainite. For austenite-to-bainite domain, it was possible to detect by dilatometry, the boundary between the upper and lower bainite.

References

1. Technical data, Erasteel Company, Research and Development Department, Tour Maine, Montparnasse, 33 avenue du Maine, 75755 Paris Cedex 15
2. C. Garcia, F.G. Caballero, C. Capdevila, and L.F. Alverez, Application of Dilatometric Analysis to the Study of Solid-Solid phase transformations in Steels, *Mater. Character.*, 2002, **48**, p 101–111
3. C. Kim, V. Biss, and W.F. Hosford, A New Procedure for Determining Volume Fraction of Primary Carbides in High-Speed and Related Tool Steels, *Metall. Trans.*, 1982, **13A**, p 185
4. E. Bischoff, H. Opielka, I. Kabyemera, and S. Karagöz, SEM-Investigation into the Quantitative Metallographical Determination of Carbides in High Speed Steels, *Prakt. Metallogr.*, 1995, **32**, p 2
5. R.A. Versaci, Stability of Carbides in M2 High Speed Steel, *J. Mater. Sci. Lett.*, 1988, **7**, p 273–275
6. G. Barreau, thèse d'etat, université de Paris Sud, Centre d'Orsay, 1982
7. L.A. Dobranski, Structure and Properties of High-Speed Steel with Wear Resistant Cases or Coating, *J. Mater. Process. Technol.*, 2001, **109**, p 44–51
8. M. Pavlickova, D. Vojech, P. Novak, J. Gemperlova, A. Gemperle, N. Zarubova, P. Lejcek, P. Jurci, and P. Stolar, Thermal Treatment of PM-Tool Steel Alloyed with Niobium, *Mater. Sci. Eng.*, 2003, **A356**, p 200–207
9. G. Delbart, A. Constant, *Les Courbes de Transformation des Aciers de Fabrication Française*, IRSID, France, 1974
10. F.G. Caballero, L.F Alvarez, C. Capdevila, and C. Garcia de Andrés, The Origin of Splitting Phenomena in the Martensitic Transformation of Stainless Steels, *Scripta Mater.*, 2003, **49**, p 315–320